Eur Radiol (2011) 21:2492–2502
DOI 10.1007/s00330-011-2207-2

CARDIAC

Accuracy and variability of right ventricular volumes and mass assessed by dual-source computed tomography: influence of slice orientation in comparison to magnetic resonance imaging

Christoph J. Jensen · Alexander Wolf · Holger C. Eberle · Michael Forsting · Kai Nassenstein · Thomas C. Lauenstein · Georg V. Sabin · Oliver Bruder · Thomas Schlosser

Received: 28 February 2011 / Revised: 7 June 2011 / Accepted: 2 July 2011 / Published online: 27 July 2011

Abstract
Objective To evaluate the accuracy and variability of right ventricular (RV) volumes and mass using dual-source computed tomography (DSCT) and the influence of slice orientation in comparison to cardiac magnetic resonance imaging (CMR).
Methods In 33 patients undergoing cardiac DSCT and CMR, RV parameters were calculated using the short-axis (DSCT, CMR) and axial orientation (DSCT). Intra- and interobserver variability were assessed by Bland-Altman analysis.
Results Short-axis orientation: RV parameters of the two techniques were not statistically different. Axial orientation: RV volumes and mass were significantly overestimated compared with short-axis parameters whereas EF was similar. The short-axis approach resulted in low variability, although the axial orientation had the least amount of intra- and interobserver variability.
Conclusion RV parameters can be more accurately assessed by DSCT compared with CMR using short-axis slice orientation. RV volumes and mass are significantly higher using axial compared with short-axis slices, whereas EF is unaffected. RV parameters derived from both approaches yield high reproducibility.

Keywords Dual-source computed tomography · Cardiac magnetic resonance imaging · Right ventricular volumes · Right ventricular mass · Reproducibility

Key Points

1. Multi-detector computed tomography with retrospective gating allows evaluation of cardiac function
2. Limited spatial and temporal resolution by less modern CT equipment biased these measurements
3. Dual-Source CT allows accurate measurements of right ventricular function without additional radiation
4. Image slice orientation influences the accuracy and reproducibility of RV measurements
5. Improved reproducibility favours axial images for serial testing and multi-centre trials

Introduction

Cardiac magnetic resonance imaging (CMR) using short-axis cine images are considered the reference standard for measurements of left and right ventricular (RV) function, volumes and mass [1–3]. However, assessment of RV volumes using short-axis CMR cine images can be challenging because of through-plane motion, and difficulty

C. J. Jensen · A. Wolf · H. C. Eberle · G. V. Sabin · O. Bruder
Department of Cardiology and Angiology,
Elisabeth Hospital Essen,
Essen, Germany

M. Forsting · K. Nassenstein · T. C. Lauenstein · T. Schlosser
Department of Diagnostic and Interventional
Radiology and Neuroradiology, University Hospital Essen,
Essen, Germany

C. J. Jensen (✉)
Duke Cardiovascular Magnetic Resonance Center,
Duke University Medical Center – 3934,
Durham, NC 27710, USA
e-mail: Christoph.Jensen@duke.edu

in distinguishing the basal boundary of the right ventricle. Inaccurate delineation of the basal boundary of the RV can lead to major discrepancies and poor reproducibility of RV parameters because of the large area of the basal part of the RV [4, 5]. Therefore, axial acquisition of images has been introduced for measuring RV volumes especially in congenital heart disease to provide good delineation of the tricuspid and the pulmonary valve [4–6]. Additionally, the improved delineation of boundaries should lead to increased reproducibility of the measurements and allow for accurate serial imaging during clinical follow-up, to detect progressive RV dilation and functional deterioration [7–9].

Unfortunately, CMR is contraindicated in patients with metal implants such as pacemakers and defibrillators or poorly tolerated in patients who cannot tolerate repetitive breath-holds and long examination times in a supine position such as those with congestive heart failure and dyspnoea.

An alternative to CMR for these patients is retrospective ECG-gated multidetector computed tomography (MDCT), which requires only a single breath-hold. MDCT has been shown to be comparable with short-axis CMR for measurements of LV and RV function [10–12]. However, because of the low temporal resolution of previous generations of MDCT end-systolic and end-diastolic volumes are difficult to assess and are often overestimated [13, 14]. Furthermore, no data exist for LV and RV parameters using axial slice orientation in MDCT.

Recently, dual-source computed tomography (DSCT) was introduced into clinical use resulting in increased temporal resolution compared with previous CT generations [11, 15, 16].

The purpose of our study was to evaluate the accuracy and variability of right ventricular volumes and mass using DSCT and to determine the influence of slice orientation in comparison to CMR.

Materials and methods

The study was carried out in accordance with the ethical standards of the institutional review board and all patients gave written informed consent before DSCT and CMR imaging. This was a retrospective, cross-sectional cohort study. All consecutive patients who were clinically referred for 1) DSCT coronary angiography to evaluate the presence and extent of coronary artery disease (CAD) and 2) CMR at our institution between January 2008 and January 2009 were considered for this study. Patients undergoing both DSCT and CMR examinations on the same day were included in this study. Patients with arrhythmia, insufficient image quality, incomplete coverage of the heart, or metallic implants were excluded from the study.

Therefore the final study population consisted of 33 patients (27 male, mean age 61.0±7.2 years).

DSCT examination

All examinations were performed on DSCT (SOMATOM Definition, Siemens Healthcare, Forchheim, Germany). A DSCT examination protocol was used with the following parameters: 64×0.6 mm collimation for both detectors, gantry rotation time of 330 ms. The pitch was automatically adjusted to the heart rate of the individual patient. To minimise radiation exposure to the patient during CT examination two different algorithms were applied:

1. The care dose4D™ algorithm (Siemens Healthcare, Forchheim, Germany), which automatically adjusts the DSCT tube voltage to individual patient size and mass.
2. The tube current modulation algorithm ("ECG pulsing", Siemens Healthcare, Forchheim, Germany) resulting in a dose reduction of 80% outside the pulsing window [17]. The pulsing window using full tube current was set to 50–80% of the R-R interval in patients with a heart rate <65 bpm and to 35–80% in patients with a heart rate >65 bpm similar to previously published studies [17, 18].

The imaging length was recorded in all patients. As proposed by the European Working Group for Guidelines on Quality Criteria in CT, the estimation of the radiation dose was performed using the dose-length product and the CDTIvol [19].

The examination protocol, including breath-holding was practiced before the examinations and all CT were performed in a craniocaudal direction during inspiratory breath-hold. All patients received 0.8 mg of isosorbide dinitrate sublingually before DSCT. Patients whose heart rates exceeded 70 bpm received metoprolol i.v. before DSCT examination [11, 20]. A cardiologist examined each patient before and after DSCT coronary angiography including vital parameters to monitor side effects. The imaging delay was determined using the test bolus technique with the region of interest placed in the ascending aorta distal to the ostium of the coronary arteries. 10 mL of contrast agent (Accupaque 300, 300 mg iodine/mL; Amersham Health Buchler, Braunschweig, Germany) were injected into an antecubital vein via an 18-gauge catheter at an injection speed of 5 mL/s followed by a saline bolus (10 mL, flow 5 mL/s). The total contrast agent dosage for DSCT coronary angiography was adapted to the calculated imaging duration. A chaser consisting of 80% saline and 20% contrast agent was flushed after contrast agent injection to ensure better opacification of the right ventricle and discrimination of the interventricular septum. The total dose of contrast medium used for the CT examination was

calculated by adding the volume of the test bolus (10 mL, 5 mL/s flow), the contrast medium for the CT coronary angiography (duration of CT data acquisition multiplied by 5 mL/s flow, with a minimum of 55 mL contrast agent) plus a 20 mL bolus of a mixture of 80% saline and 20% contrast agent, at a flow rate of 5 mL/s. After the acquisition of the isotropic 3D data sets, axial images were reconstructed for every 5% of the R-R interval (0–95%) with a slice thickness of 0.75 mm, a reconstruction increment of 0.5 mm and a typical field of view of 180×180 mm (matrix 512×512).

End-diastolic and end-systolic reconstruction windows were selected based on these axial images showing the largest and smallest left ventricular cavity areas, respectively. The raw data were transferred to a PC-based workstation (Wizard, Siemens Healthcare, Erlangen, Germany). End-diastolic and end-systolic raw data sets were reconstructed in short-axis orientation (slice thickness 6 mm, without interslice gap, Fig. 1) as well as in axial orientation to cover the heart from the diaphragm to the pulmonary bifurcation (slice thickness 6 mm, without interslice gap, Fig. 2).

CMR

Cardiac magnetic resonance imaging was performed using a 1.5 Tesla MR System (Magnetom Avanto, Siemens Healthcare, Erlangen, Germany) with a phased-array body coil. After obtaining localizing scouts, the imaging protocol consisted of breath-hold balanced steady-state free precession (SSFP) cine sequences (TrueFISP, TR 3 ms, TE 1.5 ms, FA 60°, matrix 256×208, pixel size 1.4×1.4 mm) in three long-axis views (4CV, 3CV, 2CV) and contiguous short-axis slices covering the entire right ventricle (temporal resolution between 30 and 50 ms depending on the heart rate, 6-mm slice thickness, no interslice gap, Fig. 3).

RV function analysis

Right ventricular function analysis was performed on an offline workstation (Leonardo, Siemens Healthcare) using a dedicated post-processing tool (Argus, Siemens Healthcare, Erlangen, Germany). DSCT and CMR images were analyzed by an experienced cardiologist (observer 1; 6 years of experience in CMR and 5 years of experience in cardiac CT) and radiologist (observer 2; 8 years of experience in CMR and 9 years of experience in cardiac CT) who were blinded to each other's results. In the short-axis and axial data sets, the endocardial and epicardial contours were defined by manual tracing.

1) Axial slices: In the axial DSCT data sets, the uppermost slice was defined as the slice where the first pulmonary cusp could be identified [5], whereas the most apical slice was defined as the last basal slice to contain blood volume. The RV contours were traced up to the tricuspid valve and closed by a straight line across the tricuspid valve ring.
2) Short-axis slices: For both the DSCT and CMR examinations, the most apical slice was defined as the first section of the RV with a visible lumen during the entire cardiac cycle in the short-axis images. The most basal slice was defined by the section in which the ventricular myocardium encircled 50% or more of the end-diastolic and end-systolic cavity [10, 21]. In addition, if the pulmonary valve was visible, only the portion of the right ventricular outflow tract below the level of the pulmonary valve was included in the right ventricular cavity [22]. In accordance with previously published studies, papillary muscles were considered as part of the right ventricular cavity [6, 10].

Right ventricular ejection fraction (EF), end-diastolic volume (EDV), end-systolic volume (ESV) and right

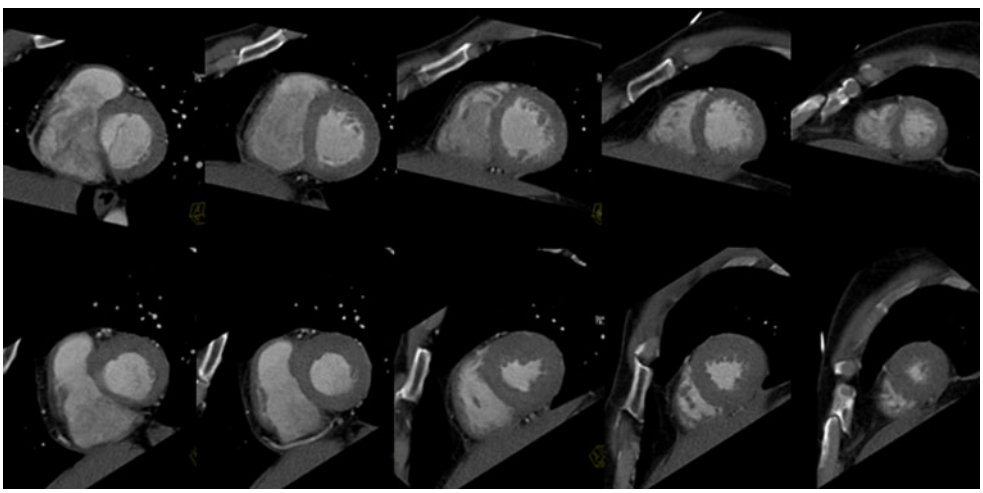

Fig. 1 Dual-source computed tomography (DSCT) images reconstructed in short-axis orientation. End-diastolic (*upper row*) and end-systolic (*lower row*) DSCT images reconstructed in short-axis orientation from base to apex (*left to right*)

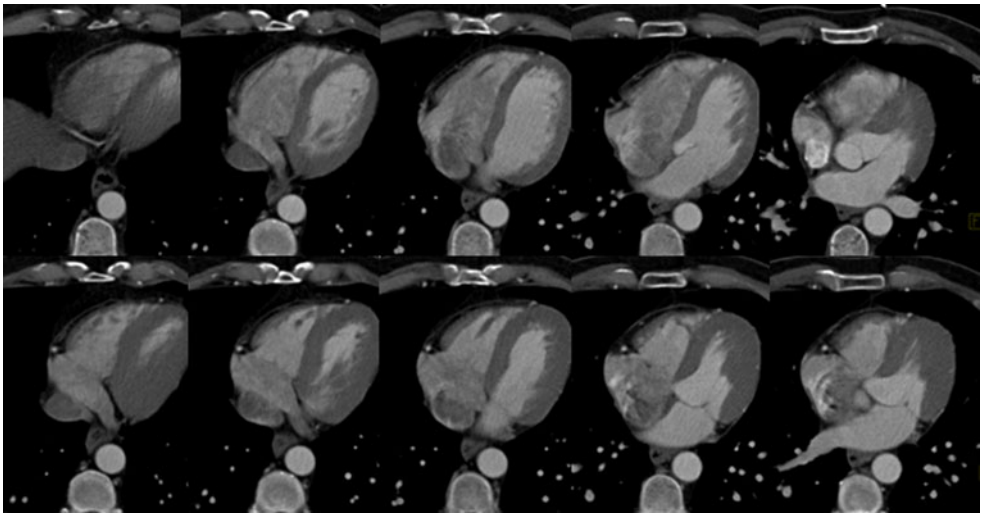

Fig. 2 Dual-source CT images reconstructed in axial orientation. End-diastolic (*upper row*) and end-systolic (*lower row*) DSCT images reconstructed in axial orientation from caudal to cranial (*left to right*)

ventricular myocardial mass (RVM) were calculated from both DSCT and CMR short-axis images and from the axial images reconstructed from DSCT by the disc summation method [22]. All data displayed are derived from measurements of observer 1 if not stated otherwise.

To avoid a recall bias, a 3-week time delay occurred between each calculation (DSCT short-axis and axial images, CMR). For intraobserver variability, studies were reanalyzed by observer 1 after an average period of 3 months. For interobserver variability, a second observer (observer 2) performed the calculation of RV parameters independently and blinded to results of observer 1.

Statistical analysis

All continuous variables were expressed as mean ± standard deviation. DSCT and CMR measurements were compared using the Wilcoxon sign rank test. Parameters displayed in Tables 1 and 2 were derived from measurements of observer 1. Bland-Altman analysis was used to display the bias (mean difference) and the 95% limits of agreement (1.96 SD around the mean difference) among the three different approaches (DSCT axial reconstruction, DSCT short-axis reconstruction, CMR short-axis acquisition) and the intra- and interobserver variability. The correlation between parameters was assessed using the Pearson's correlation coefficient. All tests were two-tailed. P values < 0.05 were considered statistically significant. All analyzes were performed with SPSS, version 13 (SPSS, Inc., Chicago, Illinois, USA).

Results

All DSCT and CMR examinations were completed successfully without the occurrence of complications. All patients of the study population fulfilled one of the following criteria: 1) atypical, stable angina, 2) ambiguous exercise stress testing, or 3) hypertensive heart disease with diagnostic ST-segment deviation in exercise stress testing but no other markers of coronary artery disease. Mean Framingham risk score was 12±8%. Additional patient

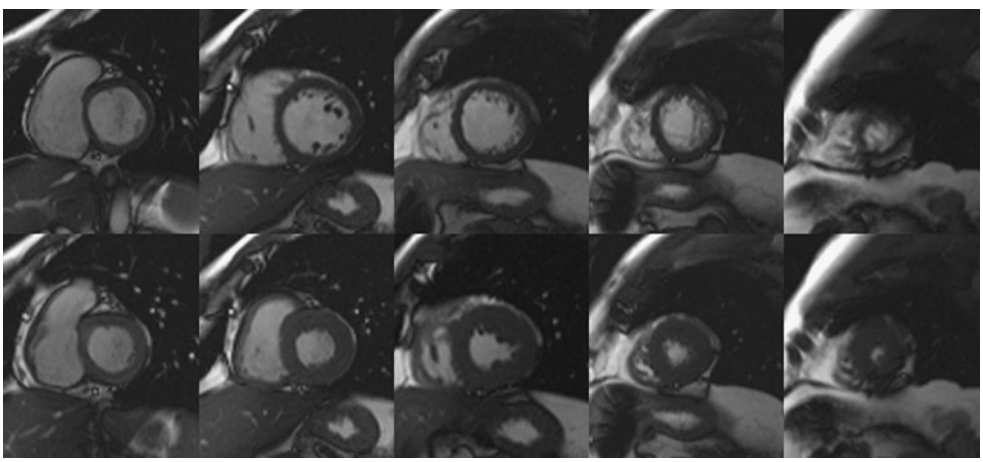

Fig. 3 Cardiac magnetic resonance (CMR) images in short-axis orientation. End-diastolic (*upper row*) and end-systolic (*lower row*) CMR short-axis images from base to apex (*left to right*)

Table 1 Patient characteristics

Parameter	
N	33
Male gender (%)	27/33 (82%)
Age (yrs)	61.0±7.2
BMI (kg/m^2)	26.7±2.8
Hypertension (%)	20/33 (60%)
Hypercholesterolemia (%)	12/33(36%)
Diabetes Mellitus (%)	4/33 (12%)
Family history of CAD (%)	5/33 (15%)
Smoking (%)	15/33 (45%)

Reported values are presented as frequencies or mean ± SD

characteristics are given in Table 1. The mean heart rate in all patients during the DSCT examination was 64±11 bpm, whereas the mean heart rate during the CMR examination was 67±10 bpm, however, the difference was not statistically significant (p=0.254). Estimated mean radiation exposure during the DSCT examinations was 7.0± 2.3 mSv. The mean time interval between DSCT and CMR examinations was 2.4±1.4 h (range 1.5–4 h).

DSCT vs. CMR

No statistically significant difference was found between DSCT and CMR when comparing the RV parameters derived from the short-axis slices (Table 2). An excellent correlation was found between DSCT and CMR values; Bland-Altman plots showed no significant variation between DSCT and CMR measurements (Fig. 4).

Short-axis vs. axial orientation in DSCT

The RV ejection fraction derived from axial and short-axis images in DSCT showed no statistically significant difference between the two slice orientations (Table 3). Conversely, RV volumes and mass were significantly higher using the axially reconstructed images compared with values derived from the short-axis orientation (Table 3). Despite excellent correlation between the measurements using axial and short-axis slice orientation, Bland-Altman plots revealed a systematic overestimation of RV EDV, ESV and mass using the axially reconstructed DSCT images (Fig.5).

Intra- and interobserver variability

The intraobserver variability is displayed in Table 4 and the interobserver variability is displayed in Table 5. The SD, and therefore the limits of agreement, in the intraobserver comparison was between 1.43 and 4.64 with a correlation coefficient between 0.875 and 0.995 (Table 3).

The interobserver analysis demonstrated higher variation for all variables compared with the intraobserver agreement. The SD, and therefore the limits of agreement, was between 3.29 and 8.34 with a correlation coefficient ranging between 0.558 and 9.81. The highest variation in the intra- and interobserver analysis was found for the RV mass in CMR and RV EDV calculated from DSCT short-axis slices.

The SD, and hence the limits of agreement, were consistently smaller for the axial method compared with the short-axis method in DSCT and CMR for both the intra- and interobserver variability. The intra- and interobserver correlation values were also higher for the axial method than for the short-axis method (Tables 4 and 5).

Discussion

In our study we compared measurements of right ventricular function and mass derived from DSCT and CMR as the reference standard. All DSCT data were obtained by DSCT coronary angiography data sets. The results from our study demonstrate that right ventricular EF, EDV, ESV and mass can be assessed accurately by DSCT using short-axis slice

Table 2 Comparison of RV parameters derived from DSCT and CMR in short-axis orientation

	RV-EF	RV-EDV	RV-ESV	RVM
DSCT mean	49.0±8.6	123.7±17.8	64.0±17.1	40.9±8.3
CMR mean	50.2±7.6	124.3±18.0	62.6±16.4	40.8±8.4
p Value	0.07	0.07	0.08	0.116
Correlation Coefficient	0.92*	0.99*	0.97*	0.99*
Mean Difference ± SD	−1.14±3.46	−0.59±1.97	1.46±3.97	0.17±0.81
Limit of Agreement	−7.92 to 5.64	−4.45 to 3.27	−6.32 to 9.24	−1.42 to 1.76

*p<0.001

Reported values are displayed as mean ± SD

RV right ventricle; *EF* ejection fraction in percent; *EDV* end-diastolic volume in mL; *ESV* end-systolic volume in mL; *RVM* right ventricular mass in g; correlation coefficient = Pearson correlation coefficient; *DSCT* dual-source computed tomography; *CMR* cardiac magnetic resonance imaging

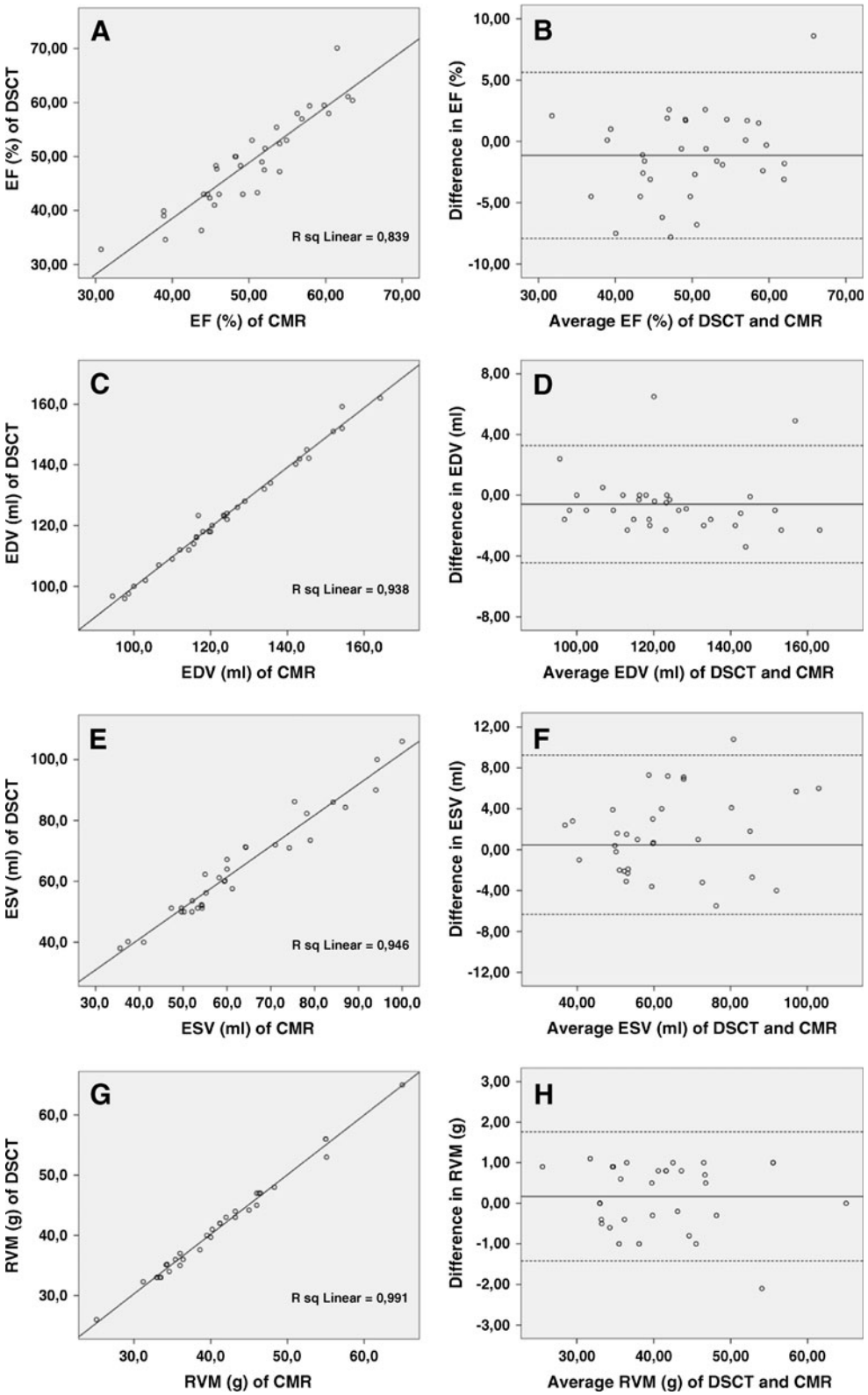

Fig. 4 Correlation of DSCT- and CMR-derived right-ventricular (RV) parameters using short-axis images (*left column*; ejection fraction (EF) (**a**), end-diastolic volume (EDV) (**c**), end-systolic volume ESV (**e**), mass (**g**). Results of Bland–Altman plot analysis (*right column*) for RV EF (**b**), EDV (**d**), ESV (**f**) and mass (**h**) assessed from short-axis images derived from DSCT and CMR. The diagrams show the difference (*y*-axis) vs. the mean values (*drawn through*) of both techniques and ±1.96-fold standard deviations (*dashed lines*)

orientation with results comparable to CMR using the same slice orientation. However, RV volumes and mass are significantly higher using axial slice orientation compared with values obtained using short-axis orientation in DSCT. Conversely, EF is unaffected by the slice orientation resulting in good agreement between measurements in

Table 3 Comparison of RV parameters calculated by short-axis and axial slices derived from DSCT

	RV-EF	RV-EDV	RV-ESV	RVM
Short-axis mean ± SD	49.0±8.6	123.7±17.8	64.0±17.1	40.9±8.3
Axial mean ± SD	49.6±7.8	133.8±19.7	68.1±18.3	43.5±8.6
p Value	0.286	<0.001	<0.001	<0.001
Correlation Coefficient	0.92*	0.96*	0.97*	0.99
Mean Difference ± SD	−0.63±3.41	−10.08±5.66	−4.06±4.84	−2.54±1.42
Limit of Agreement	−7.31 to 6.05	−21.98 to 1.01	−13.55 to 5.43	−5.32 to 0.24

*$p<0.001$

Reported values are displayed as mean ± SD

short-axis and axial orientation. Finally, high reproducibility was obtained in measuring RV volumes and mass derived from short-axis and axial slice orientations.

Right ventricular volumes, function and mass are predictive markers in a variety of cardiovascular and pulmonary diseases [13, 23, 24]. Echocardiography is widely used in clinical routine to assess the right ventricular function due to the inexpensive nature, the lack of radioactive or nephrotoxic contrast agents and the mobility of ultrasound systems [25]. However, echocardiography is operator dependent and relies on geometric assumptions using standard 2D images [25]. Additionally, imaging can be challenging due to a poor acoustic window and the geometry of the right ventricle [26]. Even 3D echocardiography has been shown to consistently underestimate RV parameters in vitro and in vivo [27]. Alternative non-invasive imaging techniques for quantifying ventricular function are radionuclide ventriculography and gated single photon emission computed tomography (SPECT). These techniques, though, are of limited availability, provide poor spatial resolution and are associated with exposing the patient to radiation [28].

For the assessment of ventricular function CMR is widely considered the standard of reference without exposing the patient to radiation [2, 27]. However, CMR can be contraindicated in patients because of implanted medical devices or might be poorly tolerated by the patient. In these patients, a reliable, highly reproducible measurement based on images acquired in one single breath-hold is most favourable. In previous studies retrospectively ECG-gated MDCT of the heart has been shown to be an efficient tool for the assessment of right and left ventricular function.

In these studies using 16-row or 64-row MDCT, overestimation of volumes in MDCT measurements was found, and was attributed to the limited temporal resolution ranging between 165 ms and 250 ms by these devices and the limited spatial resolution of 16-MDCT [10, 12, 27, 29]. Contrary to these findings, DSCT, providing an increased temporal resolution of 83 ms and a high spatial resolution comparable to that of catheter-based coronary angiography, has been shown to accurately assess LV parameters using short-axis images [11, 17, 30, 31].

To the best of our knowledge, there are no human studies assessing the capability of DSCT to measure RV volumes. RV assessment using DSCT has been performed in only two studies limited to the animal model [21, 32]. The present study confirms their observations that DSCT compared with CMR accurately depicts RV volumes and mass using SAX slice orientation. Contrary to previous published MDCT studies [12, 27], no significant difference occurred in our study comparing RV volumes calculated from SAX slices using the DSCT with those volumes calculated from CMR as the standard of reference.

Another factor influencing the accuracy of RV measurements is low contrast, which may result in inaccurate contours and poor delineation of the RV. Therefore, contrary to previous studies [14, 33] a chaser with a mixture of contrast agent and saline was used in this study to ensure better opacification and clearer delineation of the right ventricle. In our study group, which consisted of patients with suspected CAD, this chaser increased the volume of contrast agent only by 4 mL per patient. This chaser enhanced the homogeneous attenuation of the right ventricular cavity without altering coronary enhancement [18]. Especially in patients with congestive heart failure or RV dysfunction, e.g. due to pulmonary hypertension, the amount of the chaser or the contrast agent to saline ratio necessary to achieve sufficient RV attenuation might be different. Unfortunately, no systematic analysis of the absolute contrast media attenuation of the RV was performed in this study population. However, the contribution of the increased temporal resolution versus the contribution of the above-mentioned mixture of the chaser to the accuracy of DSCT-derived RV parameters compared with CMR using the short-axis orientation is not clear.

Comparing RV parameters acquired by DSCT derived from the short-axis with the values derived from axial slices, EF was almost identical in both slice orientations. But, EDV, ESV and RV mass were significantly greater derived from axial slice orientation. There may be several reasons for this finding: First, the most basal and the apical slice can be hardly defined by the short-axis method because of the poor delineation of valves and through-plane motion. Additionally, the apical segment is excluded using the short-axis method by

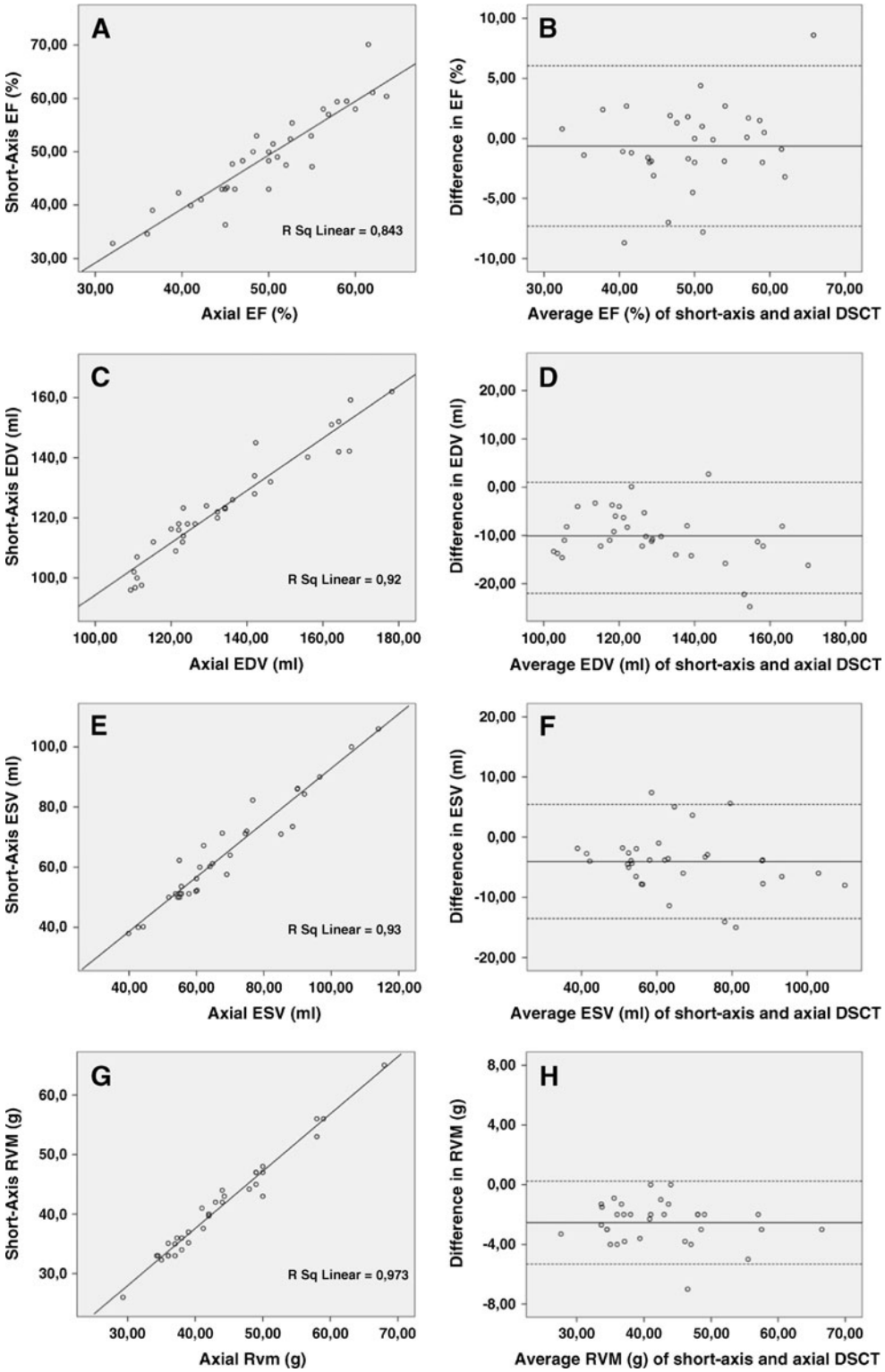

Fig. 5 Correlation of short-axis and axial reconstructed DSCT-derived RV parameters using short-axis images (*left column*; EF (**a**), EDV (**c**), ESV (**e**), mass (**g**). Results of Bland–Altman plot analysis (*right column*) for right ventricular EF (**b**), EDV (**d**), ESV (**f**) and mass (**h**) assessed from short-axis images derived from axial reconstructed and short-axis reconstructed images in DSCT. The diagrams show the difference (*y*-axis) vs. the mean values (*drawn through*) of both techniques and ±1.96-fold standard deviations (*dashed lines*)

the method's properties. On the other hand, these disadvantages are negligible using the axial slice orientation, which result in long-axis-resembling images. The axial images incorporate the apical segment into the right ventricle and provide good delineation of the basal segment because the pulmonary valve and the tricuspid valve are imaged in profile. This will result in consistently higher volumes and mass using the axial slice orientation as shown in our study.

It is difficult to compare our data with the results of previously published studies. Only two CMR studies compared axial slices with short-axis slices in patients:

Table 4 Intraobserver variability analysis

	RV-EF	RV-EDV	RV-ESV	RVM
Axial DSCT				
Bias	−0.09	−1.37	−0.59	−0.52
Limits of Agreement	−3.23 to 3.05	−5.74 to 3.00	−4.06 to 2.88	−4.85 to 3.81
SD	1.60	2.23	1.77	2.21
Correlation Coefficient	0.979*	0.994*	0.995*	0.970*
Short-Axis DSCT				
Bias	−0.36	−2.46	−0.54	−1.05
Limits of Agreement	−6.59 to 5.87	−11.55 to 6.63	−4.42 to 3.34	−3.85 to 1.75
SD	3.18	4.64	1.98	1.43
Correlation Coefficient	0.931*	0.967*	0.993*	0.986*
Short-Axis CMR				
Bias	0.21	−1.2	−0.87	−1.93
Limits of Agreement	−4.55 to 4.97	−7.75 to 5.35	−4.81 to 3.07	−9.95 to 6.09
SD	2.43	3.34	2.01	4.09
Correlation Coefficient	0.952*	0.986*	0.993*	0.875*

*$p<0.001$

Limits of agreement = 1.96 SD around the mean difference of two measurements; bias = mean difference between two measurements; axial DSCT = measurements derived from axial reconstructed images in dual-source computed tomography; short-axis DSCT = measurements derived from reconstructed images in short-axis orientation in dual-source computed tomography; short-axis CMR = measurements derived from short-axis images in cardiac magnetic resonance imaging

one in patients with repaired tetralogy of Fallot [6] and one study without congenital heart disease [5]. In the second study Alfakih et al. stated that the RV measurements derived from the axial images are systematically smaller than the values derived from short-axis images. This is contrary to our findings. These are the following reasons for this finding: In axial slices the pulmonary valve is typically seen on up to three to four slices because of the oblique position using a slice thickness of 6 mm without an interslice gap. Despite our protocol being similar to the imaging protocol proposed by Alfakih et al. the differences in image acquisition parameters can result in different slices being selected as the uppermost slice and therefore increase or decrease the calculated volume. Additionally, a recently published study using CMR comparing ventricular volumes derived from short-axis vs. axial images in patients with corrected tetralogy of Fallot reported smaller RV ESV, although higher values using axial images for RV EDV, LV EDV and LV ESV derived from axial images as well [6].

On the other hand partial volume effects of blood and myocardium could make it difficult to differentiate the blood-myocardium boundary on the acquired images. These effects are influenced by slice orientation, motion, slice thickness and spatial resolution. Theoretically, axial images are affected to a greater extent than short-axis images due to the large diaphragm part of the right ventricle, which can account for the difference in volumes and mass between the two slice orientations in our study. A small slice thickness and a high spatial resolution, as used in our study, should diminish these effects.

Table 5 Interobserver variability analysis

	RV-EF	RV-EDV	RV-ESV	RVM
Axial DSCT				
Bias	−0.14	−2.98	−1.41	−3.39
Limits of Agreement	−7.61 to 7.33	−13.76 to 6.13	−9.09 to 6.27	−9.88 to 3.09
SD	3.81	4.65	3.92	3.31
Correlation Coefficient	0.898*	0.976*	0.979*	0.938*
Short-Axis DSCT				
Bias	3.08	−3.48	−4.96	−3.39
Limits of Agreement	−5.82 to 11.98	−19.83 to 12.87	−11.41 to 1.49	−10.56 to 3.78
SD	4.54	8.34	3.29	3.66
Correlation Coefficient	0.867*	0.896*	0.981*	0.914*
Short-Axis CMR				
Bias	1.86	−4.50	−4.18	−4.38
Limits of Agreement	−9.78 to 13.50	−15.61 to 6.61	−15.57 to 7.21	−19.24 to 10.48
SD	5.94	5.67	5.81	7.58
Correlation Coefficient	0.806*	0.955*	0.943*	0.552*

*$p<0.001$

An additional finding is that reproducibility assessed by intra- and interobserver variability was excellent throughout the study and well within the clinically acceptable range. In particular, RV values using images in axial orientation were found to be more reproducible than RV parameters derived from short-axis DSCT and CMR. This confirms the previously published studies [5, 6] and indicates that the axial slice approach is best suited to consecutive follow-up studies in patients in whom accurate measurements of RV parameters or their change over time are vital. Due to the fact that these parameters derived from the axial approach are not interchangeable with the parameters derived from the short-axis approach, there is a need to establish reference values using images in axial slice orientation.

Furthermore, although not part of this study, the axial orientation theoretically increases reproducibility by means of an observer-independent slice positioning. Although it has been shown that the angle in which short-axis slices are planned, has only a small impact on left ventricular volumes, to eliminate the operator-dependent influence of slice positioning might be crucial especially in multicentre trials or serial testing [34].

Another approach to further reduce observer dependency and decrease variability could be the use of automatic software to analyze RV volumes and mass. Furthermore, the time needed to analyze RV volumes can be reduced using an automatic algorithm. A head-to-head comparison between variability and time consumption of RV measurements between manual and automatic approaches would be most welcome. Unfortunately, no recording of the time the observers spent analyzing the CMR and DSCT images was kept in our study. However, contour finding algorithms for the RV still rely heavily on observer interaction. Threshold value-supported 3D reconstructions did not show convincing results in a prior published study which was attributed to low temporal resolution and poor contrast media attenuation of the RV [14].

The need for iodinated contrast media and the radiation exposure restricts the use of DSCT as a first line method for evaluating cardiac function. For instance, in patients with implanted defibrillators and tetralogy of Fallot, CT examinations can provide reliable cardiac functional parameters and additional data on coronary anatomy. Additionally, as shown in this study, the requisite data for assessing RV function is readily available in patients who have already undergone CT coronary angiography with retrospective ECG gating for evaluation of coronary artery disease. This can improve the diagnostic significance and may alter therapeutic strategies in the individual patient.

There are limitations to our study. First, the study group was small and only patients who were referred for DSCT and CMR examination for evaluation of clinically suspected coronary heart disease were included. Whether patients underwent CMR was at the discretion of the referring physician. Therefore, a certain referral bias, which can lead to different results in patients with e.g. RV dysfunction, cannot be excluded. Second, due to the retrospective nature of this study, only CMR short-axis images were acquired for the evaluation of the right ventricular volumes. These are part of our standard CMR protocol for evaluation cardiac function, volumes and mass. However, considering the good agreement of CT and CMR short-axis derived RV parameters, we do not think that the main findings of this study are influenced by this limitation. Third, patients were given intravenous metoprolol before the DSCT examination. This premedication could change the ventricular function and volumes [11], but as each patient underwent CMR within 4 h of DSCT examination, the same interfering effects could be assumed in DSCT and CMR examination given that the half-life of i.v. administered metoprolol is 4–6 h. This is supported by the lack of a difference in recorded heart rate during the DSCT and CMR examinations, as well as the excellent accuracy of DSCT RV parameters compared with CMR parameters using the short-axis orientation.

In summary, RV volumes, function and mass using short-axis slices can be reliably assessed with high reproducibility using DSCT examinations compared with CMR. Right ventricular EF calculated from axial slice orientation in DSCT is comparable to that of CMR. RV volumes and mass derived from axial slice orientation are significantly higher compared with DSCT values derived from short-axis images. However, the observer-independent planning approach and the smaller intra- and interobserver variability, compared with the short-axis acquisition, may favour the axial orientation to calculate RV volumes and mass in multicentre studies and in patients requiring serial imaging.

References

1. Pattynama PM, De Roos A, Van der Wall EE, Van Voorthuisen AE (1994) Evaluation of cardiac function with magnetic resonance imaging. Am Heart J 128:595–607
2. Pennell DJ, Sechtem UP, Higgins CB et al (2004) Clinical indications for cardiovascular magnetic resonance (CMR): Consensus Panel Report. J Cardiovasc Magn Reson 6:727–765
3. Lyne JC, Pennell DJ (2005) Cardiovascular magnetic resonance in the quantitative assessment of left ventricular mass, volumes and contractile function. Coron Artery Dis 16:337–343
4. Remy-Jardin M, Delhaye D, Teisseire A, Hossein-Foucher C, Duhamel A, Remy J (2006) MDCT of right ventricular function: impact of methodologic approach in estimation of right ventricular ejection fraction, part 2. AJR Am J Roentgenol 187:1605–1609
5. Alfakih K, Plein S, Bloomer T, Jones T, Ridgway J, Sivananthan M (2003) Comparison of right ventricular volume measurements between axial and short axis orientation using steady-state free precession magnetic resonance imaging. J Magn Reson Imaging 18:25–32
6. Fratz S, Schuhbaeck A, Buchner C et al (2009) Comparison of accuracy of axial slices versus short-axis slices for measuring

ventricular volumes by cardiac magnetic resonance in patients with corrected tetralogy of fallot. Am J Cardiol 103:1764–1769
7. Luijnenburg SE, Robbers-Visser D, Moelker A, Vliegen HW, Mulder BJ, Helbing WA (2010) Intra-observer and interobserver variability of biventricular function, volumes and mass in patients with congenital heart disease measured by CMR imaging. Int J Cardiovasc Imaging 26:57–64
8. Sheehan FH, Kilner PJ, Sahn DJ et al (2010) Accuracy of knowledge-based reconstruction for measurement of right ventricular volume and function in patients with tetralogy of Fallot. Am J Cardiol 105:993–999
9. Moroseos T, Mitsumori L, Kerwin WS et al (2010) Comparison of Simpson's method and three-dimensional reconstruction for measurement of right ventricular volume in patients with complete or corrected transposition of the great arteries. Am J Cardiol 105:1603–1609
10. Guo YK, Gao HL, Zhang XC, Wang QL, Yang ZG, Ma ES (2010) Accuracy and reproducibility of assessing right ventricular function with 64-section multi-detector row CT: comparison with magnetic resonance imaging. Int J Cardiol 139:254–262
11. Jensen CJ, Jochims M, Hunold P et al (2010) Assessment of left ventricular function and mass in dual-source computed tomography coronary angiography: influence of beta-blockers on left ventricular function: comparison to magnetic resonance imaging. Eur J Radiol 74:484–491
12. Schlosser T, Mohrs OK, Magedanz A, Voigtlander T, Schmermund A, Barkhausen J (2007) Assessment of left ventricular function and mass in patients undergoing computed tomography (CT) coronary angiography using 64-detector-row CT: comparison to magnetic resonance imaging. Acta Radiol 48:30–35
13. Coche E, Vlassenbroek A, Roelants V et al (2005) Evaluation of biventricular ejection fraction with ECG-gated 16-slice CT: preliminary findings in acute pulmonary embolism in comparison with radionuclide ventriculography. Eur Radiol 15:1432–1440
14. Koch K, Oellig F, Oberholzer K et al (2005) Assessment of right ventricular function by 16-detector-row CT: comparison with magnetic resonance imaging. Eur Radiol 15:312–318
15. Rist C, Johnson TR, Becker A et al (2007) Dual-source cardiac CT imaging with improved temporal resolution: impact on image quality and analysis of left ventricular function. Radiologe 47 (287–290):292–284
16. Mahnken AH, Bruder H, Suess C et al (2007) Dual-source computed tomography for assessing cardiac function: a phantom study. Invest Radiol 42:491–498
17. Mahnken AH, Bruners P, Schmidt B, Bornikoel C, Flohr T, Gunther RW (2009) Left ventricular function can reliably be assessed from dual-source CT using ECG-gated tube current modulation. Invest Radiol 44:384–389
18. Pflederer T, Ho KT, Anger T et al (2009) Assessment of regional left ventricular function by dual source computed tomography: interobserver variability and validation to laevocardiography. Eur J Radiol 72:85–91
19. Hausleiter J, Meyer T, Hadamitzky M et al (2006) Radiation dose estimates from cardiac multislice computed tomography in daily practice: impact of different scanning protocols on effective dose estimates. Circulation 113:1305–1310
20. Groen JM, Greuter MJ, Schmidt B, Suess C, Vliegenthart R, Oudkerk M (2007) The influence of heart rate, slice thickness, and calcification density on calcium scores using 64-slice multi-detector computed tomography: a systematic phantom study. Invest Radiol 42:848–855
21. Bruners P, Mahnken AH, Knackstedt C et al (2007) Assessment of global left and right ventricular function using dual-source computed tomography (DSCT) in comparison to MRI: an experimental study in a porcine model. Invest Radiol 42:756–764
22. Dogan H, Kroft LJ, Huisman MV, van der Geest RJ, de Roos A (2007) Right ventricular function in patients with acute pulmonary embolism: analysis with electrocardiography-synchronized multi-detector row CT. Radiology 242:78–84
23. Oldershaw P (1992) Assessment of right ventricular function and its role in clinical practice. Br Heart J 68:12–15
24. Larose E, Ganz P, Reynolds HG et al (2007) Right ventricular dysfunction assessed by cardiovascular magnetic resonance imaging predicts poor prognosis late after myocardial infarction. J Am Coll Cardiol 49:855–862
25. Rudski LG, Lai WW, Afilalo J et al (2010) Guidelines for the echocardiographic assessment of the right heart in adults: a report from the American Society of Echocardiography endorsed by the European Association of Echocardiography, a registered branch of the European Society of Cardiology, and the Canadian Society of Echocardiography. J Am Soc Echocardiogr 23:685–713, quiz 786–688
26. Shimada YJ, Shiota M, Siegel RJ, Shiota T (2010) Accuracy of right ventricular volumes and function determined by three-dimensional echocardiography in comparison with magnetic resonance imaging: a meta-analysis study. J Am Soc Echocardiogr 23:943–953
27. Sugeng L, Mor-Avi V, Weinert L et al (2010) Multimodality comparison of quantitative volumetric analysis of the right ventricle. JACC Cardiovasc Imaging 3:10–18
28. Ramani GV, Gurm G, Dilsizian V, Park MH (2010) Noninvasive assessment of right ventricular function: will there be resurgence in radionuclide imaging techniques? Curr Cardiol Rep 12:162–169
29. Plumhans C, Muhlenbruch G, Rapaee A et al (2008) Assessment of global right ventricular function on 64-MDCT compared with MRI. AJR Am J Roentgenol 190:1358–1361
30. de Jonge GJ, van der Vleuten PA, Overbosch J et al (2010) Semi-automatic measurement of left ventricular function on dual source computed tomography using five different software tools in comparison with magnetic resonance imaging. Eur J Radiol. doi:10.1016/j.ejrad.2010.10.002
31. de Jonge GJ, van Ooijen PM, Overbosch J, Gueorguieva AL, Janssen-van der Weide MC, Oudkerk M (2010) Comparison of (semi-)automatic and manually adjusted measurements of left ventricular function in dual source computed tomography using three different software tools. Int J Cardiovasc Imaging. doi:10.1007/s10554-010-9727-8
32. Mahnken AH, Bruners P, Bornikoel CM et al (2009) Dual-source CT assessment of ventricular function in healthy and infarcted myocardium: An animal study. Eur J Radiol. doi:10.1016/j.ejrad.2009.07.037
33. Raman SV, Shah M, McCarthy B, Garcia A, Ferketich AK (2006) Multi-detector row cardiac computed tomography accurately quantifies right and left ventricular size and function compared with cardiac magnetic resonance. Am Heart J 151:736–744
34. Danilouchkine MG, van der Geest RJ, Westenberg JJ, Lelieveldt BP, Reiber JH (2005) Influence of positional and angular variation of automatically planned short-axis stacks on quantification of left ventricular dimensions and function with cardiovascular magnetic resonance. J Magn Reson Imaging 22:754–764